Supplementary Material for "Viscoelastic Necking Dynamics Between Attractive Microgels"

Shensheng Chen,[†,‡] Emad Pirhadi,[†] and Xin Yong[*,†]

†*Department of Mechanical Engineering, Binghamton University, The State University of New York, Binghamton, New York 13902, USA*

‡*Current Address: Division of Chemistry and Chemical Engineering,1200 E California Blvd, California Institute of Technology, Pasadena, California 91125, USA*

E-mail: xyong@binghamton.edu

A. Dissipative Particle Dynamics

All simulations in this work are modeled with dissipative particle dynamics (DPD). DPD is a mesoscale coarse-grained method that is widely used in polymer gel simulations[1–8] because of its computational efficiency and ability to capture hydrodynamics by simulating explicit solvents. It has also been shown to reproduce correct necking dynamics of two water droplets.[9] In DPD, each bead represents several molecules or molecules groups and its dynamics is described by Newton's second law $m\frac{d\mathbf{v}}{dt} = \mathbf{f}_i$. A DPD bead interacts with other beads through three types of pair-wise forces: $\mathbf{f}_i = \sum_j (\mathbf{F}_{ij}^C + \mathbf{F}_{ij}^D + \mathbf{F}_{ij}^R)$. The sum is carried out for all neighbor beads j within the cut-off r_0. For convenience, all DPD beads have the same mass m and cut-off interaction distance r_0, both are set to 1 per convention.[1] The conservative force is given by $\mathbf{F}_{ij}^C = a_{ij}(1 - r_{ij}/r_0)\mathbf{e}_{ij}$, where a_{ij} is the maximum repulsion

between bead i and j, $r_{ij} = |\mathbf{r}_i - \mathbf{r}_j|$ is the inter-bead distance, and $\mathbf{e}_{ij} = |r_i - r_j|/r_0$ represents the force direction. The dissipative force is related to the relative velocity between the two beads $\mathbf{v}_{ij} = \mathbf{v}_i - \mathbf{v}_i$ via $\mathbf{F}_{ij}^D = -\alpha w_D(r_{ij})(\mathbf{e}_{ij}\mathbf{v}_{ij})\mathbf{e}_{ij}$. The random force which represents a Gaussian noise is given by $\mathbf{F}_{ij}^R = \beta w_R(r_{ij})\xi_{ij}\mathbf{e}_{ij}$. Here, the random variable ξ_{ij} satisfies $\langle\xi_{ij}(t)\rangle = 0$ and $\langle\xi_{ij}(t)\xi_{kl}(t^{'})\rangle = (\delta_{ik}\delta_{jl} + \delta_{il}\delta_{jk})\delta(t - t^{'})$. The temperature of the DPD system is controlled inherently through the fluctuation-dissipation theorem, which demands $[w_R(r_{ij})]^2 = w_D(r_{ij}) = (1-r_{ij}/r_0)^2$ and $\beta^2 = 2k_{\mathrm{B}}T\alpha$, with k_{B} being the Boltzmann constant.[1] As per convention, we set $\alpha = 4.5$, and the energy scale $k_{\mathrm{B}}T$ in DPD under room temperature is also set to unity, which yields the characteristic time scale $\tau = \sqrt{mr_0^2/k_{\mathrm{B}}T} = 1$. Polymer beads are further subject to a harmonic bond potential $E_{bond} = 0.5K_{bond}(r_b - r_{b0})^2$ and an angle potential $E_{angle} = 0.5K_{angle}(1 + \cos\theta)$. The bond and angle strengths are set to $K_{bond} = 128\ k_{\mathrm{B}}T/r_0^2$ and $K_{angle} = 4\ k_{\mathrm{B}}T$, respectively. The equilibrium bond length is set to $r_{b0} = 0.5\ r_0$, θ is the angle between two consecutive bonds. The equation of motion is integrated using the velocity-Verlet algorithm. The total number density is set to 3. Simulation time step is set to $\Delta t = 0.01\ \tau$. Note that this relatively small time step is necessary for avoiding nonphysical bond crossing in DPD simulations of dense polymer systems. We test polymer melt and attractive microgel systems with the above setting, no bond crossing is observed. However, increasing $\Delta t >= 0.015\ \tau$ will results in significant bond crossing.

B. Microgel and Droplet Models

To easily control the internal network structure of microgel particles, each microgel in this work is modeled as a tetra-functional polymer network within a spherical cutoff.[3,7] A polymer strand within the microgel has N coarse-grained polymer beads. Each microgel has approximately 90,000 beads, and have a radius $R \approx 20\ r_0$ in the collapsed state. The microgel beads in DPD simulations can be mapped to physical oligomer units of poly(N-isopropylacrylamide) PNIPAM microgels. Each solvent bead in our simulations represents 12 water molecules.[5,7,10]

Thus the volume of one DPD bead is 360 Å^3. Mapping the solvent number density in DPD $\rho_{DPD} = 3\ r_0^3$ to the water density $\rho_{water} = 1$ g/cm^3 gives $r_0 \approx 1$ nm and the characteristic mass $m = 216$ Da.[5,7,10] Since all beads have the same mass in DPD, a coarse-grained polymer bead represents 1.9 N-isopropylacrylamide (NIPAM) monomers. Knowing the characteristic length and energy yields the intrinsic time scale $\tau = (mr_0^2/k_{\mathrm{B}}T)^{0.5} = 9.6$ ps. Thus, the physical radius of the attractive microgels in this work is about 20 nm assuming uniform density within the gel. We vary $N = 4, 7, 16, 30$, and 50, which yield microgels with crosslinking densities of approximately $\psi = 11\%, 7\%, 5\%, 3\%$, and 1%, respectively. Note that we remove the dangling chains at the microgel-solvent interface so all polymer strands have a uniform length. the difference in total bead number for different ψ is within 2%.

The interaction between solvent and polymers determines the microgel swelling states. We choose the repulsive parameter between like beads to be: $a_{ss} = a_{pp} = 25\ k_{\mathrm{B}}T/r_0$, with the subscripts s and p representing solvent and polymer species, respectively. The repulsive parameter between the unlike polymer and solvent beads, a_{ps} , is related to the Flory-Huggins χ_{ps} parameter characterizing the polymer-solvent interactions by $a_{ps} - 25 = \chi_{ps} k_{\mathrm{B}}T/0.306$. a_{ps} between thermal-responsive microgels (e.g., PNIPAM) with a lower critical solution temperature (LCST) and water has been investigated in our previous studies.[3,5,10] Thus, we set $a_{ps} = 32.5\ k_{\mathrm{B}}T/r_0$ in this work to yield collapsed microgels with polymer concentrations over 90%.[5,10] All microgels are initially isolated in a simulation box of 60 r_0^3 for running 1×10^6 time steps for equilibration. Two identical attractive microgels are then placed into a simulation box of 120 $r_0 \times 60\ r_0 \times 60\ r_0$. The centers of mass of the microgels align with the center line of the x axis with a small separation distance of 1 r_0 between microgel surfaces. We then bring them together with a small initial velocity of magnitude 0.01 r_0/τ, similar to experimental analysis and other simulation approach.[11]

The two reference systems of liquid droplets and polymer droplets are created in a similar way as microgels. Except that there is no bond between liquid droplet beads and no crosslinks connect polymer chains in polymer droplets. The total bead number in one droplet is similar

for all three spices ($N_{tot} \approx 90,000$). The equilibrium and necking initiation process in these two systems are the same as microgel particles. However, liquid droplets beads are more likely to diffuse into the outer fluid compared to polymeric systems, so we increase the bead-bead interaction between liquid droplets and the outer fluid to $a_{ls} = 100\ k_{\mathrm{B}}T/r_0$. All the droplets have radii of approximately 20 nm before interaction.

C. Neck Radius Calculation

We calculate the neck radius by assuming the neck as a short cylinder between the two microgels. We divide the simulation box into small spatial bins with a thickness of $\Delta x = 0.2\ r_0$ in the direction of the approaching coordinate x, and count the polymer or droplet beads in each slabs. In every 10 time steps, the minimum sum of bead count in three consecutive bins will define the location of the neck. The bead number count N_{sum} in these three bins will serve to calculated the neck radius r assuming impressibility: $\pi r^2 \cdot 3\Delta x \cdot \rho_p = N_{sum}$, where ρ_p is the polymer number density. To avoid the noise of very early time, the characterization of the neck radius begins when $r > 2.5\ r_0$, similar to the necking analysis in other simulation studies.[11] Five independent runs will be performed for one necking growth analysis. The initial time for $r = 2.5\ r_0$ is determined by interpolating the neck-evolution profiles to satisfy the condition that the necking starts in $\tau = 0$.

References

(1) Groot, R. D.; Warren, P. B. Dissipative particle dynamics: Bridging the gap between atomistic and mesoscopic simulation. *The Journal of Chemical Physics* **1997**, *107*, 4423–4435.

(2) Español, P.; Warren, P. B. Perspective: Dissipative particle dynamics. *The Journal of Chemical Physics* **2017**, *146*, 150901.

(3) Chen, S.; Yong, X. Dissipative particle dynamics modeling of hydrogel swelling by osmotic ensemble method. *The Journal of Chemical Physics* **2018**, *149*, 094904.

(4) Chen, S.; Olson, E.; Jiang, S.; Yong, X. Nanoparticle assembly modulated by polymer chain conformation in composite materials. *Nanoscale* **2020**, *12*, 14560–14572.

(5) Chen, S.; Yong, X. Elastocapillary interactions of thermoresponsive microgels across the volume phase transition temperatures. *Journal of Colloid and Interface Science* **2021**, *584*, 275–280.

(6) Chen, S.; Yong, X. Janus Nanoparticles Enable Entropy-Driven Mixing of Bicomponent Hydrogels. *Langmuir* **2019**, *35*, 14840–14848.

(7) Hoppe Alvarez, L.; Eisold, S.; Gumerov, R. A.; Strauch, M.; Rudov, A. A.; Lenssen, P.; Merhof, D.; Potemkin, I. I.; Simon, U.; Wöll, D. Deformation of Microgels at Solid–Liquid Interfaces Visualized in Three-Dimension. *Nano Letters* **2019**, *19*, 8862–8867.

(8) Camerin, F.; Gnan, N.; Rovigatti, L.; Zaccarelli, E. Modelling realistic microgels in an explicit solvent. *Scientific Reports* **2018**, *8*, 14426.

(9) Akella, V.; Gidituri, H. Universal scaling laws in droplet coalescence: A dissipative particle dynamics study. *Chemical Physics Letters* **2020**, *758*, 137917.

(10) Yong, X.; Kuksenok, O.; Matyjaszewski, K.; Balazs, A. C. Harnessing Interfacially-Active Nanorods to Regenerate Severed Polymer Gels. *Nano Letters* **2013**, *13*, 6269–6274.

(11) Perumanath, S.; Borg, M. K.; Chubynsky, M. V.; Sprittles, J. E.; Reese, J. M. Droplet Coalescence is Initiated by Thermal Motion. *Physical Review Letters* **2019**, *122*, 104501.

Supplementary Figures

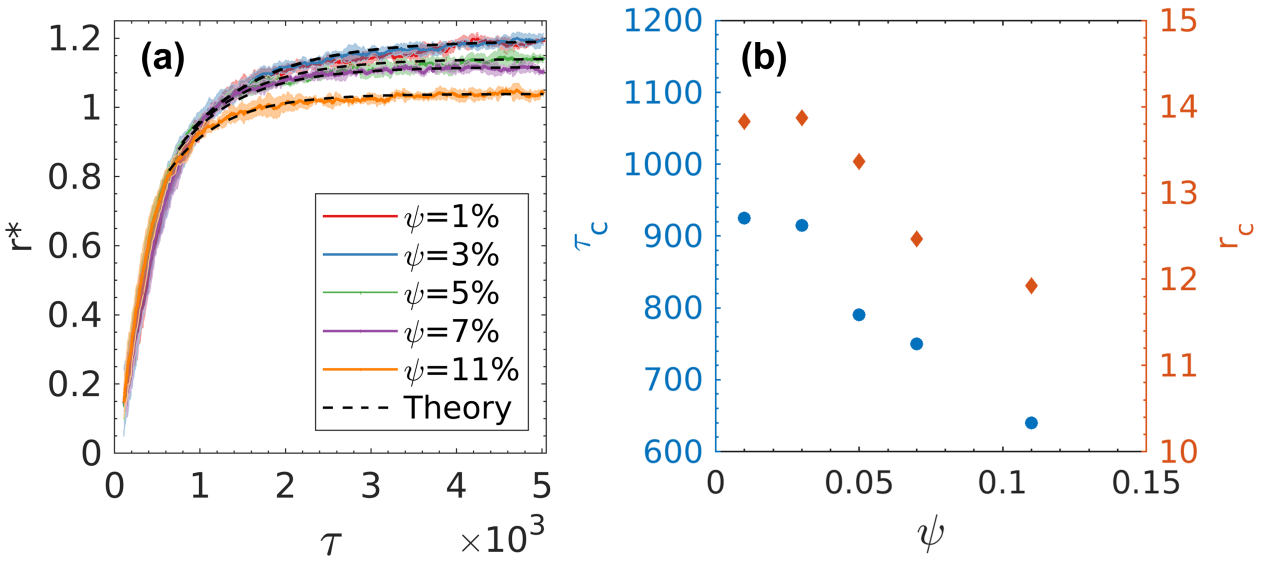

Figure S1: (a) Individual fittings of neck growth to Eq. (5) for microgels with different crosslinking densities. (b) The dependence of resulting fitting parameters: characteristic relaxation time of polymer relaxation τ_c and corresponding neck radius r_c on microgel crosslinking density.